

Original scientific paper

## EXPERIMENTAL AND NUMERICAL DETERMINATION OF THE WHEEL-RAIL ANGLE OF ATTACK

UDC 629.4

**Dragan Milković<sup>1</sup>, Goran Simić<sup>1</sup>, Jovan Tanasković<sup>1</sup>,  
Živana Jakovljević<sup>2</sup>, Vojkan Lučanin<sup>1</sup>**

<sup>1</sup>University of Belgrade Faculty of Mechanical Engineering, Rail Vehicles Department

<sup>2</sup>University of Belgrade Faculty of Mechanical Engineering, Department for Production Engineering, Serbia

**Abstract.** *Angle of attack is an important wheel-rail contact parameter. It serves for estimation of the rolling stock curving performance. Together with wheel-rail contact forces, angle of attack influences the wear index. This paper presents experimental on-track measurements of the angle of attack using a specially designed laser device installed on track. Experiments are performed on three types of rail vehicles: shunting locomotive series 631-301, motor unit 412-077 and trailing unit 416-077 of electromotor train 412/416. Experimental measurements are compared with multibody system (MBS) simulations using specialized computer package VAMPIRE Pro. We have found good agreement between the results obtained experimentally and by simulations. Using these data, we have also performed relative comparison of wear indices of the outer wheels of the leading wheelsets for each of the tested vehicles.*

**Key Words:** *Angle of Attack, Measurements, Multibody Simulations, Wear Index*

### 1. INTRODUCTION

One of the most important roles of the railway vehicle's wheelsets is to provide for safe guidance of the vehicle along track. Considering the design characteristics of the wheelsets, profiles of the wheel running treads and the rail heads as well as the design limitations of the suspension system link elements, it is almost impossible to achieve perfect radial steering of the wheelsets in sharp curves. The resulting yaw angle of the wheelset relative to the track longitudinal axis is defined as angle of attack (Fig. 1).

---

Received January 22, 2015 / Accepted April 2, 2015

**Corresponding author:** Dragan Milković

Affiliation: Faculty of Mechanical Engineering, University of Belgrade, Kraljice Marije 16, Belgrade

E-mail: dmilkovic@mas.bg.ac.rs

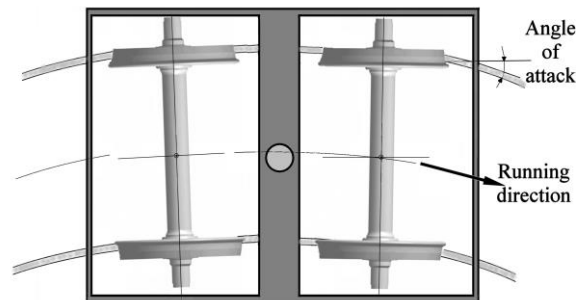


**Fig. 1** Angle of attack during curve negotiation

Criteria for estimation of the railway vehicle dynamics during curve negotiation, including derailment safety, depend on the ratio between lateral  $Y$  and vertical  $Q$  forces in the wheel-rail contact ( $Y/Q$ ), as well as on the wheel-rail angle of attack  $\alpha$  [1, 2]. These parameters together influence wear intensity expressed using wear indices [3–5]. Considering the importance of these parameters for experimental research as well as prototype testing of the railway vehicles in this paper we present a developed device for angle of attack (AOA) measurements and experimental results obtained by its use. The developed device is wayside and mobile, comparing to other devices [6, 7] that are installed on the vehicles and it can be used for measurements only on this vehicle.

In order to present possible applications of AOA measurements for wear analyses, in this paper we have included some results of contact forces measurements obtained using another developed device presented in [8]. It has turned out that the maximum performances of both devices can be achieved if they are used in parallel, in order to collect as many as possible reliable parameters for each vehicle and to compare these results with numerical simulations.

## 2. DEVICE FOR AOA MEASUREMENTS

The developed device for AOA measurements identifies position of the wheel relative to some surface or axis using a Micro-Epsilon optoNCDT 1700 laser device (Fig. 2).



**Fig. 2** Laser device positioning relative to the rail

The angle between the wheel and the defined reference, which represents longitudinal rail axis, defines wheel-rail AOA -  $\alpha$ . Considering the laser's accuracy and the measurement principle, this device should be positioned perpendicularly to the rail longitudinal direction. Perpendicularity verification is done by means of the device itself, by recording the laser-to-rail distance while sliding from one guide end to the other.

### 3. IN-SITU MEASUREMENTS OF THE AOA

In this paper we present characteristic results recorded for shunting locomotive 621-301 and electromotor unit 412/416.

Immediately before measurements, the laser beam direction was checked relative to the rail (Fig. 3). It appeared that deviation of the laser beam from the perpendicular was 12.4 mrad ( $0.71^\circ$ ). According to analysis performed in [9], such a small deviation has negligible influence on the measurement accuracy (less than  $\pm 1\%$ ), so it was not necessary to correct the laser position.

In order to present the method for data processing, as an example in this paper we present complete results of measurements performed on electromotor train's trailing unit 416-077.



**Fig. 3** Trailing unit EMU 416-077– AOA measurement device without protective cover

Fig. 4 presents laser-obtained recording of passing of the leading and the trailing wheelsets and the position of the outer wheels relative to rail.

For obtaining the wheel-rail AOA, the recorded data were transformed from the time domain to the spatial one by using the measured train speed. The speed was measured by using the device itself based on the laser record in time  $L$  and the known distance between two adjacent wheelsets (wheelbase) of the tested vehicles passing by the laser. To avoid influence of the wheelsets distance on speed measurement, it is also possible to use a separate device with two switches installed on predefined (known) distance on the track, activated by the wheel passing for speed measurements. We used the device itself considering influence of the wheelset distance with tolerances and the maximum sampling rate of the laser 2500 Hz.

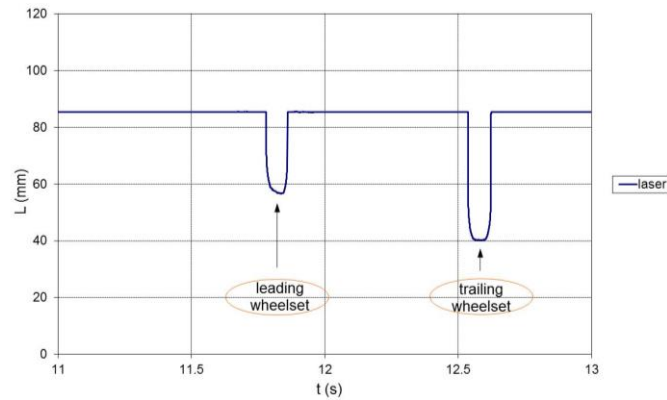


**Fig. 4** Trailing unit EMU 416-077 outer wheels – recorded data

In the case of the maximum expected speed of 100 km/h during curve negotiation (for the curve radius of 400 m and the maximum allowable unbalanced acceleration) and the minimum wheelbase distance  $p = 1.8$  m (for the standard freight bogie), relative error will be 0.18%. Passing of each of the two outer wheels in spatial domain after transformation are presented in Figs. 5 and 6. From these diagrams AOA and the wheel position relative to rail can be derived. AOA  $\alpha$  is estimated based on the linear regression slope of the central segment of the recorded line with 100 mm length, which is far enough from rounded zones caused by flange passing by the laser.

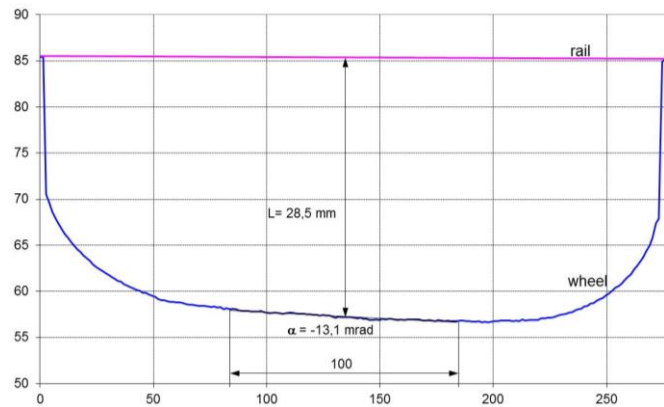


**Fig. 5** Trailing unit EMU 416-077 outer wheels – recorded data

Measured AOA was  $\alpha = -13.1$  mrad for outer wheel of the leading wheelset and  $\alpha = 1.0$  mrad for the outer wheel of the second wheelset. Relative position between the back surface of the outer wheel and the side of the outer rail in the mid position of the wheel, defined as distance between wheel and the rail measured at 10 mm below TOR (top of rail), was 28.5 mm for the leading wheelset and 45.0 mm for the second wheelset of the leading bogie.

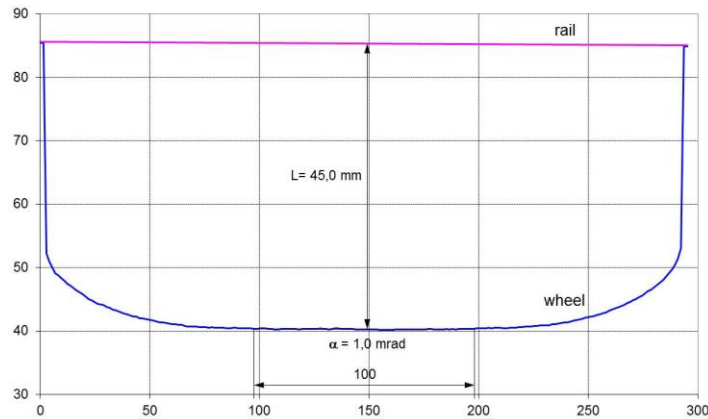


**Fig. 6** Trailing unit EMU 416-077 – relative position and AOA of the outer wheel of the second wheelset

### 3.1. Wheel-rail wear indices

All three vehicles, shunting locomotive, trailing and motor unit of EMU, were tested under the similar or almost the same conditions (same location) and all vehicles, while passing over the measurement section, were pushed, hauled, or with turned off traction. In this subsection we present relative comparison of the wear characteristics of the outer wheels of the leading wheelsets for each of the tested vehicles.

For comparison, different authors have defined different wear characteristics, which are called wear indices. Starting from expressions for wear index given in [3], which includes work of tangential forces in the wheel-rail contact, for comparison of the wear characteristics of the different vehicles with different wheel profiles, with some approximations, we used product of lateral force and AOA according to the following expression:

$$R.W.I. = k \cdot Y \cdot \xi_y = k \cdot Y \cdot \frac{V_y}{V} = k \cdot Y \cdot \alpha \quad (1)$$

where:  $k$  – constant,  $Y$  – measured lateral force,  $\xi_y$  – creepage in lateral direction,  $V_y$  – speed component in lateral direction of the wheelset,  $V$  – speed of the wheel forward movement,  $\alpha$  – AOA.

Relation between creepage  $\xi_y$  and AOA  $\alpha$  was established based on kinematics and geometric relation shown in Fig. 7. Approximation and assumption based on which expression (1) was derived were:

- Creepage represents the ratio between speed component in the creep direction and speed of the wheel forward movement,
- During curve negotiation with turned off traction, wear is influenced dominantly by tangential force action in lateral direction.

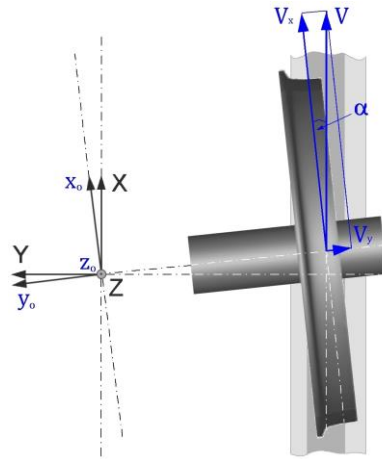


**Fig. 7** Creepage in lateral direction

The obtained results of the relative wear index for the three tested vehicles are presented in Tab. 1. As a reference vehicle for comparison we have selected shunting locomotive as the vehicle with the least favourable wear performances.

**Table 1** Relative wear index *R.W.I.* of the tested vehicles

	$V$ (km/h)	$Y$ (N)	$ \alpha $ (mrad)	$Y \cdot \alpha$ (N·rad)	Relative wear index <i>R.W.I.</i>
Shunting locomotive 631-301	13	26900	16.6	446.54	1.00
Motor unit 412-077	14	23300	14.7	342.51	0.77
Trailing unit 416-077	13	15400	13.1	201.74	0.45

Based on the results presented in Table 1 it can be seen that the shunting locomotive has the highest wear index. This is an expected result since the shunting locomotive has the largest axle load (18 t), no bogies, and an axle distance of 3 m, comparing to EMU 412/416 with 2.6 m axle distance and with rigid axle guidance (radial steering). By comparing results for the trailing and motor unit of the electromotor train, it can be seen that there is a significant difference in calculated wear indices, although both vehicles have the same axle distance and the same bogie distance. The difference comes: 1) from the larger mass of motor unit wheelsets, for having installed axle transmission, 2) due to larger mass of the bogies, caused by mass of traction motors and total larger mass of the motor unit carbody, and 3) due to differences in the installed equipment. Radial steering of both vehicles is similar and almost fully rigid, which is in accordance with close measured values of angles of AOA:  $-13.1$  mrad for trailing, and  $-14.7$  mrad for motor unit. Relative comparison between three tested vehicles shows that trailing unit 416-077 has the lowest value of the AOA and the best wear performance.

#### 4. NUMERICAL ANALYSIS

Simulation of the railway vehicle dynamics using some of the specialized computer simulation packages may also serve as a good design tool. Depending on the scope of an analysis, it can have very detailed vehicle models and, at the same time, it can include some simplifications of the track model, such as considering it either as rigid or as installed on uniform elastic foundation. Some research works [10, 11] focus on the track analysis using 2D models, while the excitation influence of the vehicle is approximated using some simplified vehicle models. There are also simulations [12–14] that consider vehicles and tracks as a multibody system (MBS), while considering only vertical vehicle/track interaction.

In our research, we have used computer programme Vampire Pro [15] for a curving analysis during passing through the sharp curve with a 214 m radius, on the track without superelevation, excluding the influence of any other track geometric imperfections.

Due to the lack of available data on input parameters for all vehicles, we have performed simulation only for electromotor trailing unit for which we had available data on suspension elements stiffness, dumping characteristics, as well as on the axle guiding stiffness.

Below we present an overview of the performed simulations and obtained results. Fig. 8 shows a non-linear model of the EMU series 412/416 indicating detail of one bogie with suspension elements. Bogie frame and wheelsets are presented transparently in order to provide for a better overview of the suspension system and link elements.

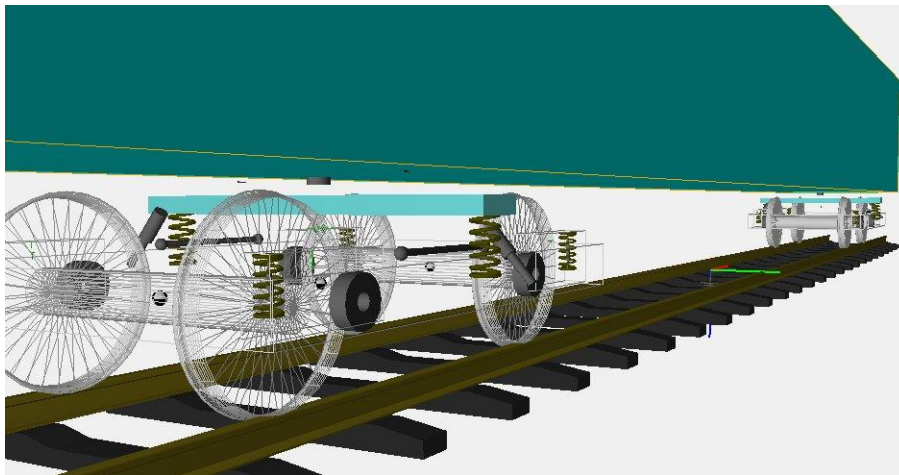


**Fig. 8** Model of EMU [9]

Vampire Pro allows for linear stiffness and damping terms to be specified between the rail and the sleeper, and sleeper-to-ground as shown in Fig. 9. Damping terms are not important for a quasi-static curving analysis. In this case they just support convergence of the simulations results. The most significant track stiffness terms used in the simulations are adopted from Ref. [15]. They are: the lateral rail to the sleeper stiffness 43 kN/mm, the lateral sleeper to the ground stiffness 37 kN/mm, and the vertical sleeper to the ground stiffness 50 kN/mm. The rails and sleepers are considered to be massless degrees of freedom, which is appropriate for the steady-state curving analysis.

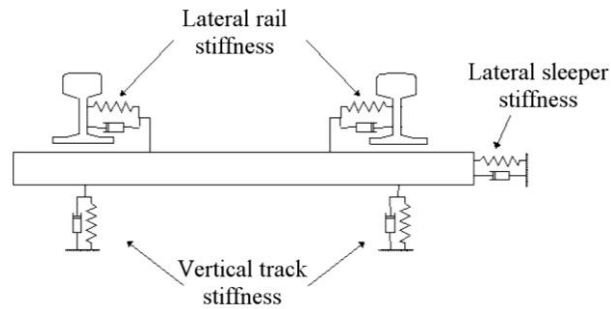


**Fig. 9** Track model [15]

All the vehicle parameters used in the simulation are selected based either on performed measurements, or from available technical documentation.

For the modelling of the wheel-rail contact, Non-Linear Creep law is used. This creep law uses a pre-calculated contact data table that describes the contact data parameters with respect to wheelset lateral shift across the track at rail level. For that purpose real wheel and rail profile data measured using profilometer are used as input for the computation of the actual creep forces.

The results of steady-state curving analysis have shown fairly good agreement having in mind strong dependence of the simulation results on various input parameters of the simulation model. Although this programme was benchmarked during several internationally recognized benchmarking exercises and the results have shown fairly good agreement [16], the simulation results should be interpreted with caution.

From the analyses performed on the trailing unit of the electromotor train 412/416, it can be seen that AOA of the leading wheelset obtained by simulation is  $-12.0$  mrad while the experimental result is  $-13.1$  mrad. AOA of the second wheelset of the trailing unit obtained using simulation is  $-0.5$  mrad, and the corresponding measured value is  $1.0$  mrad.

## 5. CONCLUSIONS

The presented results show that a specially designed laser system installed on the track is able to measure accurately the lateral wheel offset, the vehicle speed, and angle of attack  $\alpha$ .

For the selected measurement principle, the speed of the passing vehicle is the most important - yet still low - influence on the accuracy of  $\alpha$  measurement. The high accuracy is possible if the perpendicularity between the laser beam and the rail longitudinal axis is kept within  $\pm 5^\circ$ , which is relatively easy to achieve.

Additionally, the obtained results are used for mutual validation of the experimental measurements and the results of the multibody system (MBS) simulations. It has turned out that there exists good agreement between these results, which further encourages experimental research in the railway vehicle dynamics using the presented measurement system. Also the comparison of the results shows that, provided the accurate track stiffness parameters are used, vehicle dynamics simulations can predict angle of attack with sufficient accuracy.

**Acknowledgements:** *The authors express their gratitude to the Ministry of Education, Science and Technological Development, Republic of Serbia research grant TR 35045 and TR 35006.*

#### REFERENCES

1. EN 14363 *Railway applications - Testing for the acceptance of running characteristics of railway vehicles - Testing of running behavior and stationary tests*, June, 2005.
2. Guan Q., Zeng J., Jin X., 2014, *An angle of attack-based derailment criterion for wheel flange climbing*, Proc IMechE Part F: J Rail and Rapid Transit, 228, pp. 719-729.
3. Kumar S., Prasana Rao D.L., 1984, *Wheel-Rail Contact Wear, Work, and Lateral Force for Zero Angle of Attack—A Laboratory Study*, Journal of Dynamic Systems, Measurement and Control, 106, pp. 319-326.
4. Pombo J., Ambrosio J., Pereira M., Lewis R., Dwyer-Joyce R., Ariaudo C., Kuka N., 2011, *Development of a wear prediction tool for steel railway wheels using three alternative wear functions*, Wear, 271, pp. 238-245.
5. Santamaria J., Vadillo E.G., Oyarzabal O., 2009, *Wheel-rail wear index prediction considering multiple contact patches*, Wear, 267, pp. 1100-1104.
6. Iijima H., Horioka K., Kataori A., Momosaki S., Doi K., 2011, *Development of Continuous Measurement Equipment for Angle of Attack and Results of Measurements*, JR East Technical Review, 19, pp. 46-49.
7. Sugiyama H., Tanii Y., Suda Y., Nishina M., Komine H., Miyamoto T., Doi H., Chen H., 2011, *Wheel/rail contact geometry on tight radius curved track: simulation and experimental validation*, Multibody Syst Dyn, 25, pp. 117-130.
8. Milković D., Simić G., Jakovljević Ž., Tanasković J., Lučanin V., 2013, *Wayside systems for wheel-rail contact forces measurements*, Measurement, 46, pp. 3308-3318.
9. Milković D., 2012, *The influence of wheel-rail contact parameters on railway vehicle dynamic behaviour* (in Serbian), Doctoral Dissertation, University of Belgrade, Faculty of Mechanical Engineering, Belgrade, 172 pp.
10. Grassie S.L., 1992, *A contribution to dynamic design of railway track*, Vehicle System Dynamics, 20, pp. 195-209.
11. Kerr A.D., 2000, *On the determination of the rail support modulus k*, International Journal of Solids and Structures, 37, pp. 4335-4351.
12. Ripke B., Knothe K., 1995, *Simulation of high frequency vehicle-track interactions*, Vehicle System Dynamics, 24, pp. 72-85.
13. Sun Y. Q., Dhanasekar M. A., 2002, *A dynamic model for the vertical interaction of the rail track and wagon system*, International Journal of Solids and Structures, 39, pp. 1337-1359.
14. Zhai W., Sun X., 1994, *A Detailed Model for Investigating Vertical Interaction between Railway Vehicle and Track*, Vehicle System Dynamics, 23, pp. 603- 615.
15. VAMPIRE® Pro Version 5.50 Programme, DeltaRail Group Ltd., Derby 2011.
16. Iwnicki S. (Ed.), 1999, *The Manchester Benchmarks for Rail Vehicles Simulation*, Supplement to Vehicle System Dynamics, CRC Press, p. 206.